



## Charm–anticharm baryon production asymmetries in photon–nucleon interactions

FOCUS Collaboration<sup>1</sup>

J.M. Link<sup>a</sup>, P.M. Yager<sup>a</sup>, J.C. Anjos<sup>b</sup>, I. Bediaga<sup>b</sup>, C. Göbel<sup>b</sup>, A.A. Machado<sup>b</sup>,  
J. Magnin<sup>b</sup>, A. Massafferri<sup>b</sup>, J.M. de Miranda<sup>b</sup>, I.M. Pepe<sup>b</sup>, E. Polycarpo<sup>b</sup>,  
A.C. dos Reis<sup>b</sup>, S. Carrillo<sup>c</sup>, E. Casimiro<sup>c</sup>, E. Cuautle<sup>c</sup>, A. Sánchez-Hernández<sup>c</sup>,  
F. Vázquez<sup>c</sup>, C. Uribe<sup>d</sup>, L. Agostino<sup>e</sup>, L. Cinquini<sup>e</sup>, J.P. Cumalat<sup>e</sup>, B. O'Reilly<sup>e</sup>,  
I. Segoni<sup>e</sup>, M. Wahl<sup>e</sup>, J.N. Butler<sup>f</sup>, H.W.K. Cheung<sup>f</sup>, G. Chiodini<sup>f</sup>, I. Gaines<sup>f</sup>,  
P.H. Garbincius<sup>f</sup>, L.A. Garren<sup>f</sup>, E. Gottschalk<sup>f</sup>, P.H. Kasper<sup>f</sup>, A.E. Kreymer<sup>f</sup>,  
R. Kutschke<sup>f</sup>, M. Wang<sup>f</sup>, L. Benussi<sup>g</sup>, M. Bertani<sup>g</sup>, S. Bianco<sup>g</sup>, F.L. Fabbri<sup>g</sup>,  
A. Zallo<sup>g</sup>, M. Reyes<sup>h</sup>, C. Cawfield<sup>i</sup>, D.Y. Kim<sup>i</sup>, A. Rahimi<sup>i</sup>, J. Wiss<sup>i</sup>, R. Gardner<sup>j</sup>,  
A. Kryemadhi<sup>j</sup>, Y.S. Chung<sup>k</sup>, J.S. Kang<sup>k</sup>, B.R. Ko<sup>k</sup>, J.W. Kwak<sup>k</sup>, K.B. Lee<sup>k</sup>, K. Cho<sup>l</sup>,  
H. Park<sup>l</sup>, G. Alimonti<sup>m</sup>, S. Barberis<sup>m</sup>, M. Boschini<sup>m</sup>, A. Cerutti<sup>m</sup>, P. D'Angelo<sup>m</sup>,  
M. DiCorato<sup>m</sup>, P. Dini<sup>m</sup>, L. Edera<sup>m</sup>, S. Erba<sup>m</sup>, M. Giammarchi<sup>m</sup>, P. Inzani<sup>m</sup>,  
F. Leveraro<sup>m</sup>, S. Malvezzi<sup>m</sup>, D. Menasce<sup>m</sup>, M. Mezzadri<sup>m</sup>, L. Moroni<sup>m</sup>, D. Pedrini<sup>m</sup>,  
C. Pontoglio<sup>m</sup>, F. Prelz<sup>m</sup>, M. Rovere<sup>m</sup>, S. Sala<sup>m</sup>, T.F. Davenport III<sup>n</sup>, V. Arena<sup>o</sup>,  
G. Boca<sup>o</sup>, G. Bonomi<sup>o</sup>, G. Gianini<sup>o</sup>, G. Liguori<sup>o</sup>, M.M. Merlo<sup>o</sup>, D. Pantea<sup>o</sup>,  
D. Lopes Pegna<sup>o</sup>, S.P. Ratti<sup>o</sup>, C. Riccardi<sup>o</sup>, P. Vitulo<sup>o</sup>, H. Hernandez<sup>p</sup>, A.M. Lopez<sup>p</sup>,  
E. Luiggi<sup>p</sup>, H. Mendez<sup>p</sup>, A. Paris<sup>p</sup>, J.E. Ramirez<sup>p</sup>, Y. Zhang<sup>p</sup>, J.R. Wilson<sup>q</sup>,  
T. Handler<sup>r</sup>, R. Mitchell<sup>r</sup>, D. Engh<sup>s</sup>, M. Hosack<sup>s</sup>, W.E. Johns<sup>s</sup>, M. Nehring<sup>s</sup>,  
P.D. Sheldon<sup>s</sup>, K. Stenson<sup>s</sup>, E.W. Vaandering<sup>s</sup>, M. Webster<sup>s</sup>, M. Sheaff<sup>t</sup>

<sup>a</sup> University of California, Davis, CA 95616, USA

<sup>b</sup> Centro Brasileiro de Pesquisas Físicas, Rio de Janeiro, RJ, Brazil

<sup>c</sup> CINVESTAV, 07000 México City, DF, Mexico

<sup>d</sup> IFUAP, 72570 Puebla, Mexico

<sup>e</sup> University of Colorado, Boulder, CO 80309, USA

<sup>f</sup> Fermi National Accelerator Laboratory, Batavia, IL 60510, USA

<sup>g</sup> Laboratori Nazionali di Frascati dell'INFN, I-00044 Frascati, Italy

<sup>h</sup> University of Guanajuato, 37150 Leon, Guanajuato, Mexico

<sup>i</sup> University of Illinois, Urbana-Champaign, IL 61801, USA

<sup>j</sup> Indiana University, Bloomington, IN 47405, USA

<sup>k</sup> Korea University, Seoul 136-701, South Korea

<sup>l</sup> Kyungpook National University, Taegu 702-701, South Korea

<sup>m</sup> INFN and University of Milano, Milano, Italy

<sup>n</sup> University of North Carolina, Asheville, NC 28804, USA

<sup>o</sup> Dipartimento di Fisica Nucleare e Teorica and INFN, Pavia, Italy

<sup>p</sup> University of Puerto Rico, Mayaguez, PR 00681, USA

<sup>q</sup> University of South Carolina, Columbia, SC 29208, USA

<sup>r</sup> University of Tennessee, Knoxville, TN 37996, USA

<sup>s</sup> Vanderbilt University, Nashville, TN 37235, USA

<sup>t</sup> University of Wisconsin, Madison, WI 53706, USA

Received 26 November 2003; accepted 3 December 2003

Editor: M. Doser

---

## Abstract

We report measurements of the charm–anticharm production asymmetries for  $\Lambda_c^+$ ,  $\Sigma_c^{++}$ ,  $\Sigma_c^0$ ,  $\Sigma_c^{++*}$ ,  $\Sigma_c^{0*}$ , and  $\Lambda_c^+(2625)$  baryons from the Fermilab photoproduction experiment FOCUS (E831). These asymmetries are integrated over the region where the spectrometer has good acceptance. In addition, we have obtained results for the photoproduction asymmetries of the  $\Lambda_c$  baryons as functions of  $p_L$ ,  $p_T^2$ , and  $x_F$ . The integrated asymmetry for  $\Lambda_c^+$  production,  $(\sigma_{\Lambda_c^+} - \sigma_{\Lambda_c^-})/(\sigma_{\Lambda_c^+} + \sigma_{\Lambda_c^-})$ , is  $0.111 \pm 0.018 \pm 0.012$ , significantly different from zero. The asymmetries of the excited states are consistent with the  $\Lambda_c$  asymmetry.

© 2004 Published by Elsevier B.V. Open access under [CC BY license](#).

---

The FOCUS experiment uses a photon beam on a beryllium oxide target to produce charm particles. In high energy photon–hadron interactions, pairs of charm–anticharm quarks are produced predominantly through photon–gluon fusion [1]. At leading order in quantum chromodynamics (QCD), the produced charm and anticharm particles are identically distributed in the kinematic variables. At next-to-leading order, small asymmetries are expected between charm and anticharm production [2–4]. However, these predicted asymmetries would be too small to be measured at the current level of experimental statistics. Interactions between the produced charm quarks and those in the struck nucleon during hadronization can also induce production asymmetries. One common model is that of string fragmentation as implemented in PYTHIA [5]. In this model, the charm and anticharm quarks are connected through color strings to the quarks in the struck nucleon. The energy in these strings is converted to particles by “popping”  $q\bar{q}$  pairs out of the vacuum. The simplest asymmetry example occurs when a charm quark is connected to the diquark in the nucleon by a low energy string with insufficient energy to produce any additional particles. In this case, the charm quark can combine with valence  $u$  and  $d$

quarks to form a  $\Lambda_c$  while a  $\bar{c}$  quark can only form mesons when it combines with the valence quarks.

In this Letter we present a high-statistics measurement of the production asymmetry of  $\Lambda_c$  baryons from photon–nucleon interactions, providing the first convincing evidence for a non-zero asymmetry. This Letter also contains the first measurements of this asymmetry as functions of  $p_L$ ,  $p_T^2$ , and  $x_F$ . In addition, the production asymmetries of the excited charm baryons  $\Sigma_c^{++}$ ,  $\Sigma_c^0$ ,  $\Sigma_c^{++*}$ ,  $\Sigma_c^{0*}$ , and  $\Lambda_c^+(2625)$  are presented for the first time. All of these states decay to a  $\Lambda_c$  plus one or two charged pions.

The FOCUS (Fermilab E831) experiment was designed to study charm particle physics. Charmed hadrons are produced by the interaction of high energy photons ( $\langle E \rangle \approx 175$  GeV for events in which a charm decay was reconstructed) with a segmented beryllium oxide (BeO) target. The photons are produced by bremsstrahlung in a lead target with a 300 GeV  $e^+/e^-$  beam. Vertex reconstruction is performed using four silicon strip planes interleaved with segments of the target followed by a 12 plane silicon strip vertex detector. Downstream of the vertex detector, tracking and momentum measurements are made using five stations of multiwire proportional chambers and two large aperture magnets with opposite polarity. Three multicell Čerenkov counters operating in threshold mode are used to identify electrons, pions, kaons, and protons over a wide range of momenta. The spectrom-

---

<sup>1</sup> See <http://www-focus.fnal.gov/authors.html> for additional author information.

eter also contains a hadron calorimeter, two electromagnetic calorimeters, and two muon detectors. Data were collected during the 1996–1997 fixed-target run.

The  $\Lambda_c^+$  particles are reconstructed using the  $pK^-\pi^+$  decay mode.<sup>2</sup> The decay vertex is formed from three charged tracks in the event. The vector sum of their momenta is projected back toward the target and used as a *seed* to intersect with at least one other track in the event to form a production vertex. We require the production and decay vertices to be separated by at least  $5.5\sigma_\ell$ , where  $\sigma_\ell$  is the uncertainty in the measured vertex separation. We also place goodness-of-fit criteria on the primary and secondary vertices, requiring that the confidence level for each vertex be greater than 1%. Identification of the decay tracks by particle type is performed using the Čerenkov detector system [6]. A  $\chi^2$ -like variable is formed using the on/off status of all cells within a particle's Čerenkov cone ( $\beta = 1$ ). For each of the four possibilities, electron, pion, kaon, and proton, we calculate  $W_i = -2\sum_j^{\text{cells}} \log P_j$ , where  $i$  is the particle type and  $j$  the cell number.  $P_j$  is the probability that the  $j$ th cell will yield the observed response given particle type  $i$ . Identification is then based on differences in the  $W_i$ . The proton candidate is required to have the proton hypothesis favored over the kaon and pion hypotheses by 1 and 4 units of log likelihood, respectively. The kaon hypothesis for the kaon candidate is required to be favored over the pion hypothesis by 3 such units. For the pion candidate, the pion hypothesis cannot be disfavored by more than 6 units of log likelihood relative to the most likely hypothesis. This very loose requirement is also applied to the pions from the excited charm decays, described below. To remove longer lived charm backgrounds, the lifetime of the  $\Lambda_c$  in its rest frame must be shorter than 8 times the world average lifetime [7].  $\Lambda_c$  candidates are identified as all those events which satisfy the above criteria and which fall into the mass range between 2.10 and 2.45 GeV/ $c^2$ . Finally, we restrict our sample to be in the (large) phase space region given by  $40 < p_L < 200$  GeV/ $c$  and  $p_T^2 < 6.0$  (GeV/ $c$ )<sup>2</sup>.

The  $\Sigma_c^{++}$ ,  $\Sigma_c^0$ ,  $\Sigma_c^{++*}$ , and  $\Sigma_c^{0*}$  candidates are reconstructed by combining the  $\Lambda_c^+$  candidates within  $2\sigma$  of the mean  $\Lambda_c^+$  mass with a single charged pion

track. All possible combinations in the event are tried. The confidence level of the  $\Sigma_c$  decay vertex is required to be greater than 1%. To reduce systematic errors coming from the reconstruction of the  $\Lambda_c^+$  and obtain better signal-to-noise, we study the  $\Sigma_c$  states using the difference in the invariant mass of each  $\Sigma_c$  state and the invariant mass of the  $\Lambda_c^+$ ,  $\Delta M$ . Because the pion is typically of low momentum, it suffers from a considerable amount of multiple scattering, and the uncertainty on its momentum dominates the error on the  $\Sigma_c$  invariant mass. To improve the momentum measurement, the primary vertex is refit without this *soft* pion track (if possible), and the pion direction is recomputed, forcing it to come from the refit primary.

$\Lambda_c^+$  (2625) candidates are reconstructed by combining the  $\Lambda_c^+$  candidates within  $2\sigma$  of the mean  $\Lambda_c^+$  mass with all combinations of two pions of opposite charge in the event. As for the  $\Sigma_c$  states, we use the mass difference plots and force the two pions to come from the primary.

FOCUS data were taken with three different beam energies and with two different radiators. Since the asymmetries can depend on the energy spectrum of the incident beam photons, we include only those events in our sample that come from data taken with a 300 GeV  $e^-/e^+$  beam on a lead radiator of 20% of a radiation length. This selection results in a charm baryon yield which is about 75% of the yield found using all of the data. For reconstructed charm events passing the trigger, the beam energy is reasonably well described by a Gaussian with mean of 175 GeV and width of 45 GeV.

From studies of high statistics meson decays we find no evidence that there is any asymmetry introduced by charge bias in the spectrometer. Even so, since the acceptance depends on the longitudinal and transverse momenta of the produced baryon state, if these spectra are different for particle and antiparticle over the range for which the asymmetry is measured, there will be an acceptance difference for the two samples which can be corrected. This corrected asymmetry gives the asymmetry for an experiment with flat acceptance in  $p_L$  and  $p_T^2$  over the range  $40 < p_L < 200$  GeV/ $c$  and  $p_T^2 < 6.0$  (GeV/ $c$ )<sup>2</sup>.

To compensate for this acceptance difference as a function of  $p_T^2$  and  $p_L$ , the production asymmetry  $A$  is determined by:

<sup>2</sup> Charge conjugate states are implied, unless stated otherwise.

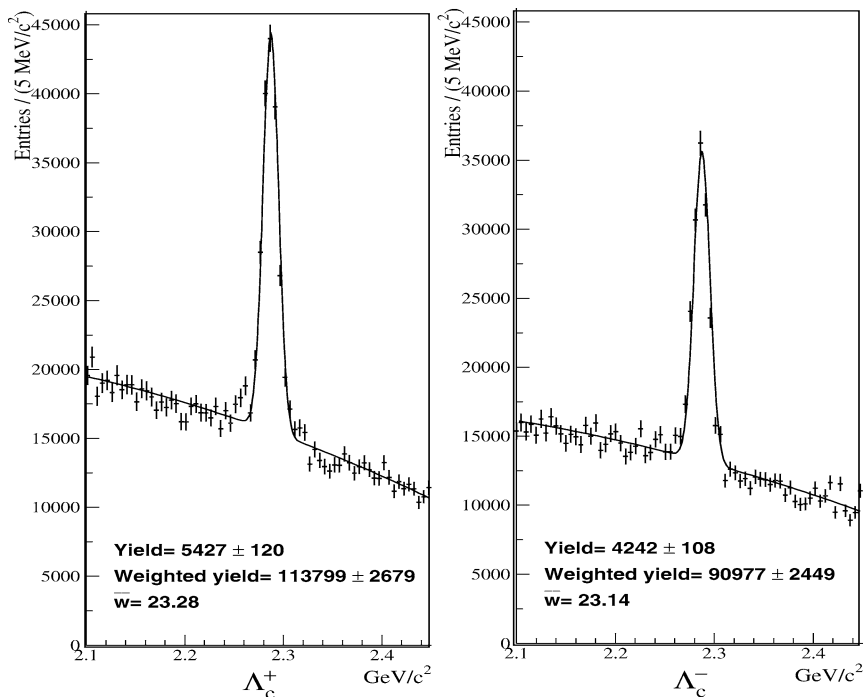


Fig. 1.  $pK^-\pi^+$  weighted invariant mass distribution split by charge. The weights are used to account for efficiency loss versus momentum on an event-by-event basis. The average weight for the whole histogram is given in the figure as  $\bar{w}$ . The unweighted yields are also shown.

$$A = \frac{N/\epsilon - \bar{N}/\bar{\epsilon}}{N/\epsilon + \bar{N}/\bar{\epsilon}}, \quad (1)$$

where  $N$  and  $\bar{N}$  are the numbers of reconstructed baryons and antibaryons, respectively, and  $\epsilon$  ( $\bar{\epsilon}$ ) is the baryon (antibaryon) reconstruction efficiency. The efficiencies  $\epsilon$  and  $\bar{\epsilon}$  are calculated using the FOCUS Monte Carlo simulation program. The detector simulation uses a detailed description of the FOCUS detector. The physics processes are generated using PYTHIA (version 6.127), with many PYTHIA parameters tuned to match the observed FOCUS physics distributions. The remaining discrepancy between data and Monte Carlo is removed by weighting Monte Carlo events to exactly match the observed data  $p_L$  and  $p_T^2$  distributions. For the excited charm states, the particle/antiparticle efficiencies are used to correct the asymmetry. For the higher statistics  $\Lambda_c$  decays a further step is taken. Since very little  $p_T^2$  dependence on efficiency is observed, the Monte Carlo events are used to obtain the efficiency variation versus  $p_L$ . This efficiency is fit to a function which is then used to weight each event.

The global  $\Lambda_c$  asymmetry is obtained by fitting each of the two weighted invariant mass data distributions shown in Fig. 1 with a Gaussian signal and quadratic background. The Gaussian mean and width are allowed to float separately for  $\Lambda_c^+$  and  $\Lambda_c^-$ . The unweighted yields for  $\Lambda_c^+$  and  $\Lambda_c^-$  are  $5427 \pm 120$  and  $4242 \pm 108$ , respectively.

To account for natural widths and changing resolutions, the excited charm baryon states are fit slightly differently. The Monte Carlo is used to generate the signal shape which is fit to a spline function. This spline function, properly normalized, is used as the signal shape for the data, with the mass allowed to float. The advantage in the case of the  $\Sigma_c$ , and  $\Sigma_c^*$  is that the spline function is able to account for the detector resolution and natural width of the state. For the  $\Lambda_c^*$  state, the spline function is a better model of the detector resolution than a Gaussian due to the small phase space. The background shapes for  $\Sigma_c$ ,  $\Sigma_c^*$  and  $\Lambda_c(2625)$  are a threshold function  $N(1 + \alpha(\Delta M - m_\pi)\Delta M^\beta)$ , quadratic polynomial, and linear polynomial, respectively. The fits to each data sample are shown on the corresponding data plots in Figs. 2–6.

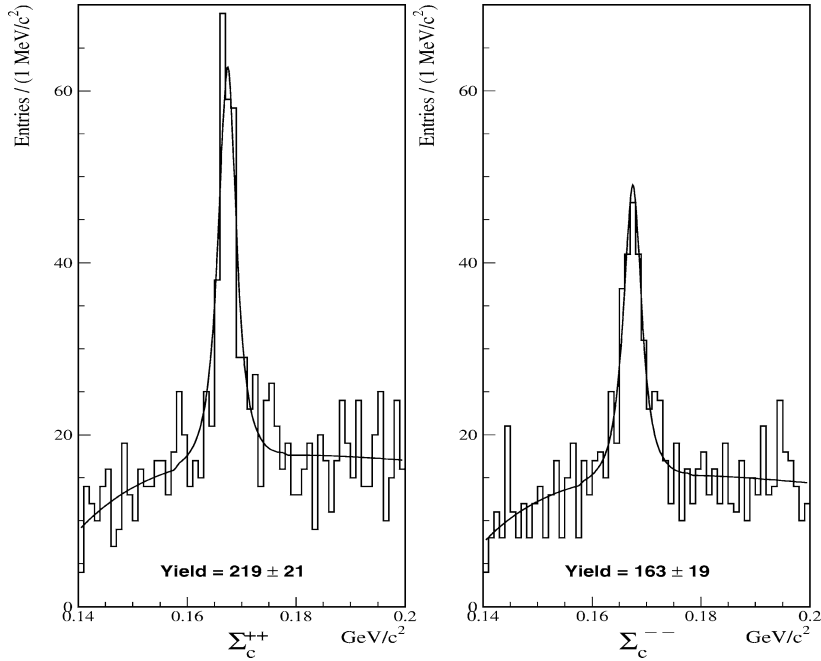


Fig. 2.  $\Lambda_c^+ \pi^+$  invariant mass distribution split by charge.

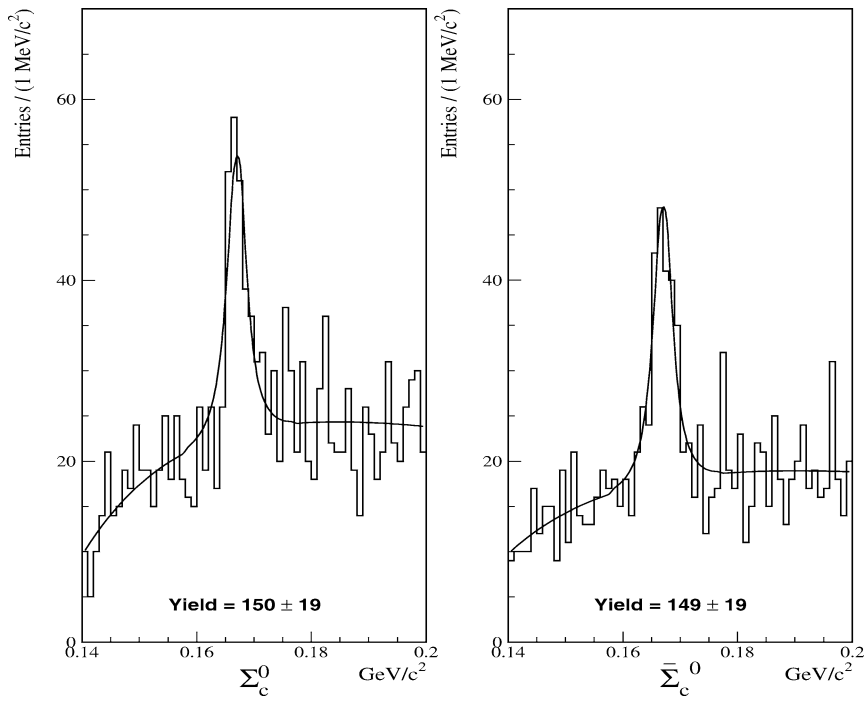
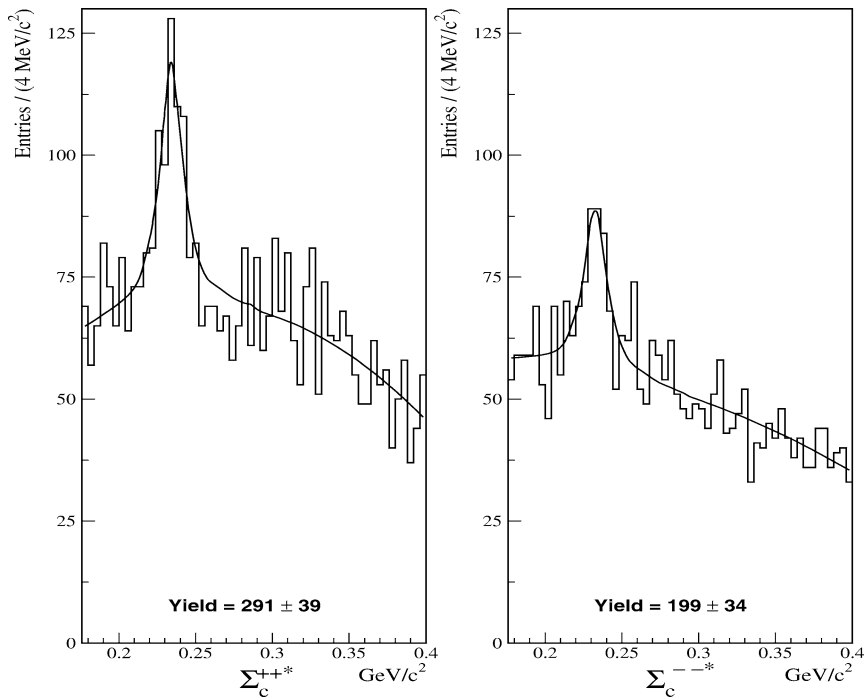
The global asymmetries are calculated from the returned yields.

The  $\Lambda_c$  data samples are divided into bins of each of the kinematic variables  $p_L$ ,  $p_T^2$ , and  $x_F$ , integrating over the full range of the other variables. The mass plots for each bin are fit using a Gaussian signal and quadratic background, as for the full data set. For these fits, the  $\Lambda_c^+$  ( $\Lambda_c^-$ ) mass is fixed to the mass obtained by fitting the full  $\Lambda_c^+$  ( $\Lambda_c^-$ ) sample. The widths are fixed to follow the Monte Carlo widths for each bin. The yields from these fits are used to obtain the production asymmetry versus  $p_L$ ,  $p_T^2$ , and  $x_F$ . The efficiency corrected asymmetry distributions for  $\Lambda_c$  vs  $p_L$ ,  $p_T^2$ , and  $x_F$  are shown in Figs. 7, 8, and 9. The  $x_F$  measurement requires knowledge of the incoming beam energy which is only available in about 30% of the data sample and is therefore of lower statistics.

In our first systematic error check, background studies were performed to assure that feedthrough from other charm states does not contribute to the asymmetry. The systematic errors are obtained by making the same measurements under different analysis conditions. We performed these studies for the global asymmetry and the asymmetry versus the kinematic variables reported.

For the  $\Lambda_c$  and the three excited states ( $\Sigma_c$ ,  $\Sigma_c^*$ , and  $\Lambda_c^*$ ), fits with different bin widths and with bins shifted by 1/2 bin were performed. A variation which fixed the mass for baryons and antibaryons to the value from the total sample was also studied. We also investigated differences due to the fit functions used. For the  $\Sigma_c$  states a Gaussian function with a quadratic background was utilized to fit the signals. For the  $\Sigma_c^*$  mass distributions we used a linear and cubic fit for the background instead of the quadratic background. For  $\Sigma_c$  and  $\Sigma_c^*$ , fits with spline functions from two additional Monte Carlo samples where the natural widths were varied by  $\pm 1\sigma$  were used to estimate the uncertainty in the knowledge of the natural widths. For the  $\Lambda_c^*$  we used two different fit functions to provide a systematic check: a Gaussian for the signal shape and a linear background and the  $\Lambda_c^*$  spline function with a quadratic background. Additionally, for all the states we used the respective raw asymmetries to check for systematic problems with the efficiency correction. For the  $\Lambda_c$  we also calculated the asymmetry using the efficiencies directly from the Monte Carlo instead of using the Monte Carlo to obtain an efficiency function.

The r.m.s. of all of these variations is used as an estimate of the systematic error.

Fig. 3.  $\Lambda_c^+ \pi^-$  invariant mass distribution split by charge.Fig. 4.  $\Lambda_c^+ \pi^+$  invariant mass distribution split by charge.

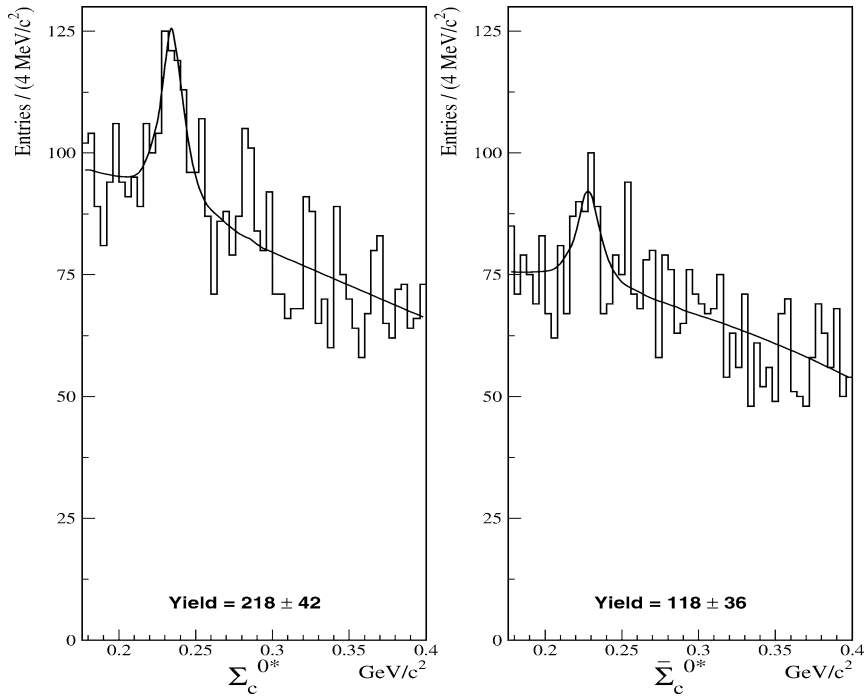


Fig. 5.  $\Lambda_c^+ \pi^-$  invariant mass distribution split by charge.

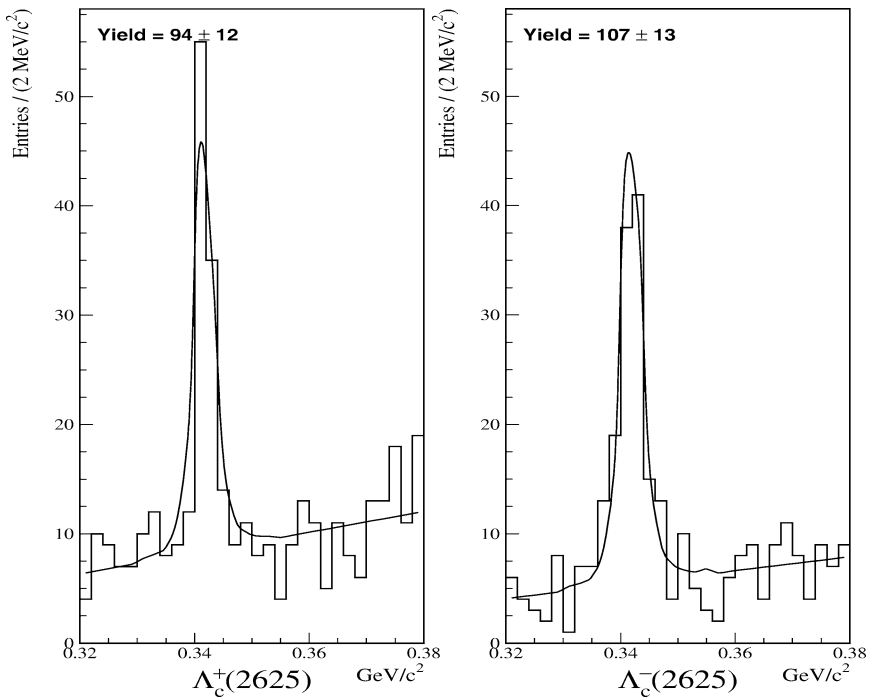


Fig. 6.  $\Lambda_c^+ \pi^+ \pi^-$  invariant mass distribution split by charge.

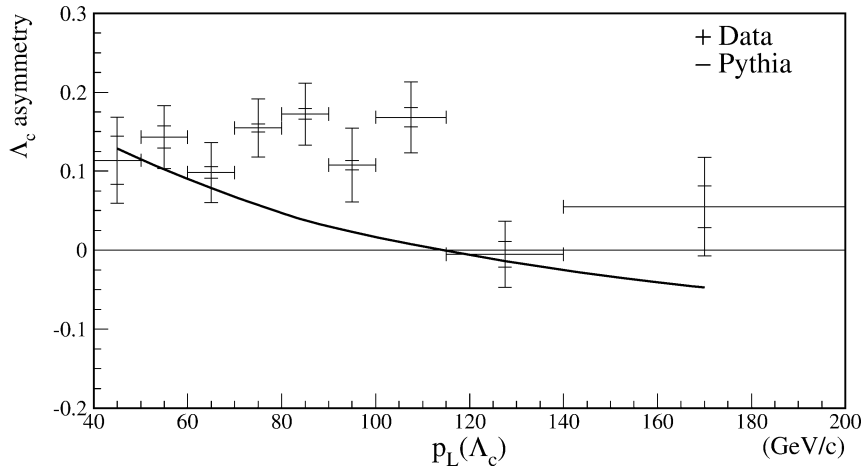


Fig. 7.  $p_L$  asymmetry distribution for  $\Lambda_c$  along with statistical and systematic errors and the PYTHIA prediction—the systematic errors are superposed on the statistical errors and are smaller than the statistical errors in every bin.

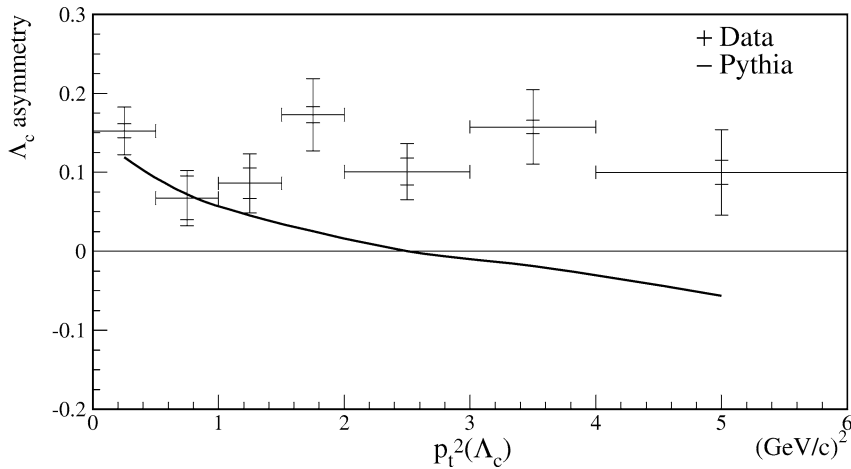


Fig. 8.  $p_T^2$  asymmetry distribution for  $\Lambda_c$  along with statistical and systematic errors and the PYTHIA prediction—the systematic errors are superposed on the statistical errors and are smaller than the statistical errors in every bin.

The global asymmetries for all of the charm baryons studied in this analysis are shown in Table 1. The first errors are statistical and the second are systematic. Table 1 also shows comparisons to PYTHIA asymmetries calculated with unreconstructed events. The PYTHIA predictions come from running version 6.203 with all parameters left at the default setting. The events are generated with the correct beam energy distribution and only candidates within the nominal phase space,  $40 < p_L < 200$  GeV/c and  $p_T^2 < 6.0$  (GeV/c)<sup>2</sup>, are used in determining the asymmetry. The E691 and E687 photoproduction experiments

have previously reported global asymmetries for  $\Lambda_c$  of  $0.110 \pm 0.089$  [8] and  $0.035 \pm 0.076$  [9], respectively. Our results are similar to those obtained by these experiments although comparisons are not straightforward since all three experiments have different phase space and beam energy distributions. Table 1 also shows the efficiency ratios of particles to antiparticles for the charm baryons studied.

We have studied the photoproduction asymmetry of  $\Lambda_c^+$  versus  $\Lambda_c^-$  using the decay channel  $pK^-\pi^+$ . From  $\sim 10\,000$   $\Lambda_c$  events we present the first results of this asymmetry as functions of  $p_L$ ,  $p_T^2$ , and  $x_F$ . These



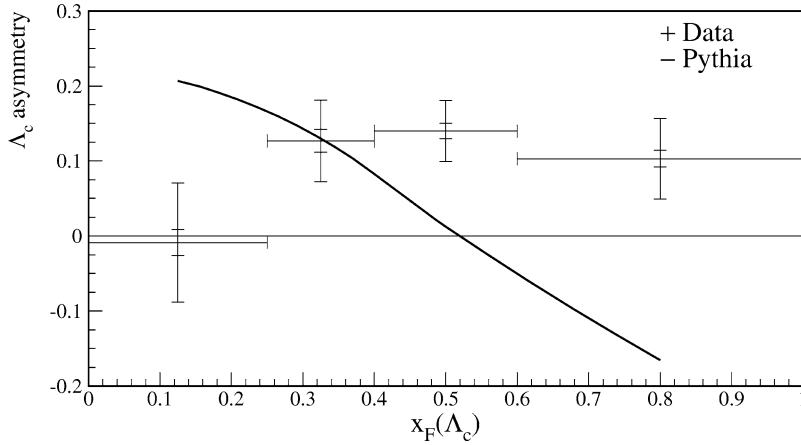


Fig. 9.  $x_F$  asymmetry distribution for  $\Lambda_c$  along with statistical and systematic errors and the PYTHIA prediction—the systematic errors are superposed on the statistical errors and are smaller than the statistical errors in every bin.

Table 1

Raw and corrected global production asymmetry for the charm baryons compared to the predictions of default PYTHIA version 6.203. The efficiency ratio of particles to antiparticles is also shown

Baryon	Raw asymmetry	Corrected asymmetry	PYTHIA	Efficiency ratio
$\Lambda_c^+$	$0.123 \pm 0.017$	$0.111 \pm 0.018 \pm 0.012$	0.073	$1.023 \pm 0.005$
$\Sigma_c^{++}$	$0.147 \pm 0.073$	$0.136 \pm 0.073 \pm 0.036$	0.126	$1.024 \pm 0.010$
$\Sigma_c^0$	$0.005 \pm 0.089$	$0.005 \pm 0.089 \pm 0.024$	0.128	$1.000 \pm 0.009$
$\Sigma_c^{++*}$	$0.188 \pm 0.105$	$0.181 \pm 0.105 \pm 0.033$	0.133	$1.016 \pm 0.006$
$\Sigma_c^{0*}$	$0.299 \pm 0.165$	$0.298 \pm 0.165 \pm 0.023$	0.132	$1.002 \pm 0.006$
$\Lambda_c^+(2625)$	$-0.066 \pm 0.086$	$-0.075 \pm 0.087 \pm 0.021$	N/A	$1.019 \pm 0.017$

results show a clear positive asymmetry. The global  $\Lambda_c^+$  asymmetry is measured to be  $0.111 \pm 0.018 \pm 0.012$ .

The production asymmetry of excited charm states which decay to  $\Lambda_c^+$ , including the  $\Sigma_c^{++}$ ,  $\Sigma_c^0$ ,  $\Sigma_c^{++*}$ ,  $\Sigma_c^{0*}$ , and  $\Lambda_c^+(2625)$  was also measured for the first time. The measurements generally indicate a positive asymmetry similar to the  $\Lambda_c$ . Because of the smaller sample size, however, they are also consistent with zero.

We find that the string fragmentation model as implemented in PYTHIA version 6.203 does not describe the  $\Lambda_c^+$  asymmetry dependence on  $p_L$ ,  $p_T^2$ , or  $x_F$ . Our measurements indicate that the asymmetry shows no significant dependence in these variables.

## Acknowledgements

We acknowledge the assistance of the staffs of Fermi National Accelerator Laboratory, the INFN of

Italy, the physics departments of the collaborating institutions and the Instituto de Física “Luis Rivera Terrazas” de la Benemérita Universidad Autónoma de Puebla (IFUAP), México. This research was supported in part by the US National Science Foundation, the US Department of Energy, the Italian Istituto Nazionale di Fisica Nucleare and Ministero della Istruzione, Università e Ricerca, Organización de los Estados Americanos (OEA), IFUAP-México, CONACyT-México, the Brazilian Conselho Nacional de Desenvolvimento Científico e Tecnológico, the Korean Ministry of Education, and the Korean Science and Engineering Foundation.

## References

- [1] L.M. Jones, H.W. Wyld, Phys. Rev. D 17 (1978) 759.
- [2] R.K. Ellis, P. Nason, Nucl. Phys. B 312 (1989) 551.
- [3] J. Smith, W.L. van Neerven, Nucl. Phys. B 374 (1992) 36.

- [4] S. Frixione, M. Mangano, P. Nason, G. Ridolfi, Nucl. Phys. B 412 (1994) 225.
- [5] T. Sjöstrand, et al., Comput. Phys. Commun. 135 (2001) 238.
- [6] FOCUS Collaboration, J.M. Link, et al., Nucl. Instrum. Methods A 484 (2002) 270.
- [7] Particle Data Group, K. Hagiwara, et al., Phys. Rev. D 66 (2002) 010001.
- [8] E691 Collaboration, J.C. Anjos, et al., Phys. Rev. Lett. 62 (1989) 513.
- [9] E687 Collaboration, P.L. Frabetti, et al., Phys. Lett. B 370 (1996) 222.